USE OF AVIRIS SPECTRAL DATA TO DISCRIMINATE MIXED PHYTOPLANKTON COMMUNITIES, SEAGRASS BEDS, AND BENTHIC ALGAL MATS IN FLORIDA BAY, USA

Laurie L. Richardson[1] and Fred A. Kruse[2]

1. INTRODUCTION

The use of hyperspectral remote sensing as a tool for scientific investigations at a regional scale has been developed to a much greater extent in the fields of geology and terrestrial biology than for aquatic ecosystems (see previous AVIRIS workshop proceedings). This is true despite the fact that a substantial amount of published data exists concerning the spectral reflectance signatures of substances (both biotic and abiotic) found in aquatic environments. These data include studies that document the spectral signatures and shifts associated with different concentrations of phytoplankton-associated chlorophyll *a* in surface waters (Gitelson ,1992; Rundquist et al., 1996; Schalles et al., 1998); the spectral reflectance signatures of differing concentrations and types of suspended sediments (Goodin et al., 1993); and the effect of mixed chlorophyll *a* and suspended sediments on overall spectral reflectance (Han et al., 1994; Schalles et al., 1997). Another line of spectral based research focuses on detecting the spectral reflectance signatures of algal accessory pigments. This approach, based on the taxonomic specificity of algal pigments (Rowan, 1989), has been used successfully to demonstrate the optically based distinction between different types of phytoplankton (Dekker et al., 1992a,b; Richardson et al., 1994; Richardson, 1996).

The different spectral reflectance signatures of algal accessory pigments are based on different functional light absorbing characteristics of individual pigments. These spectral signatures are particularly useful for hyperspectral imaging sensor data analysis in aquatic applications because the specific signatures can be used to support the classification and mapping of different types of phytoplankton assemblages. While this approach has been considered for some time (Prieur and Sathyendranath , 1981), and the theoretical basis for implementation has been advanced in terms of hyperspecral data in recent years (Dekker and Hoogenboom, 1996; Kruse et al., 1997), it is only very recently that this application has been realized using hyperspectral (AVIRIS) regional data (Richardson and Kruse, 1999). This latter work has shown that AVIRIS data can discriminate between different phytoplankton assemblages that are present in sub-basins of Florida Bay, specifically phytoplankton blooms dominated by diatoms, cyanobacteria, and green microalgae.

The capability of AVIRIS data to discriminate and map phytoplankton community structure is possible due to spectral based data analysis of AVIRIS imagery. The spectral analysis approach has extended the use of aquatic remote sensing beyond the traditional detection of chlorophyll *a* (a pigment common to all algae) in an overall approach that parallels that used by geologists in remote sensing of minerals based on their spectral signatures (Kruse et al., 1997). The aquatic application can be extended further to discriminate phytoplankton from other aquatic photosynthetic organisms that also contain chlorophyll *a*. Such an effort cannot be successfully carried out using data from sensors such as SeaWiFS that were specifically designed to detect the 433 nm absorbance feature of chlorophyll *a* because such sensors cannot distinguish between algal, seagrass (or benthic macroalgal) associated chlorophyll *a* (Stumpf et al., 1999). Hyperspectral data, on the other hand, offer spectral information in addition to the 433 nm signal, including the capability to detect a second chlorophyll *a* signal - a peak near 700 nm - that both shifts and becomes more pronounced as chl *a* concentrations in near surface waters increase (Gitelson, 1992; Rundquist et al., 1996). This particular signal is obscured by any overlying water column due to absorbance by water itself.

We report here the use of AVIRIS data to discriminate between seagrass, phytoplankton, and benthic algal mats in Florida Bay, and extend our previous work on discrimination of different phytoplankton assemblages.

[1]Florida International University, Miami, Florida (richardl@fiu.edu)
[2]Analytical Imaging and Geophysics LLC, Boulder, Colorado (kruse@aigllc.com)

2. METHODS

2 .1 Field Site.

Our field site, Florida Bay, USA, is located to the south of the Florida peninsula and to the west and north of the Florida Keys. The bay has been our experimental field site for an investigation into the use of AVIRIS data in aquatic applications for a number of years, and is described in detail elsewhere (Richardson and Zimba,2000). The feature that makes this an exceptional research site is the fact that the bay consists of a number of discrete sub-basins (both optically clear and optically dense) that are characterized by different, distinctive phytoplankton blooms. Seagrass beds are also present.

2.2 AVIRIS Data and Groundtruthing.

Eleven AVIRIS scenes were acquired of Florida Bay on March 23, 1996. On this date AVIRIS was flown on NASA's ER-2 high-altitude aircraft to yield scenes that were 10 by 12 km with 20m pixels. The eleven scenes were acquired in three separate runs that imaged most of the central, northern, and eastern bay. During AVIRIS data acquisition groundtruth sampling (for algal accessory pigments) was conducted from a small boat in seven sub-basins of the bay. The groundtruth data set, which consists of a suite of accessory pigments measured using HPLC, has been described previously (Richardson and Kruse, 1999; Richardson and Zimba, 2000).

Two of the eleven scenes were selected for a study aimed at discriminating seagrass, benthic algal mats, and different phytoplankton assemblages. The two scenes represent very different areas of Florida Bay. One of these (run 5, scene 2) is a nearshore (north central) area of the bay that images a portion of the wetlands ecosystem located at the southern tip of the Florida peninsula. This scene contains the sub-basin Rankin, one of the seven AVIRIS flight groundtruth basins. Rankin consistently exhibits optically dense phytoplankton blooms and high concentrations of suspended sediment. (Suspended sediments were not measured in the groundtruth field work.) Part of the bay in the Rankin image exhibits extremely shallow (<1 m) areas. Discrete basins ranging from >1 to 2 m are also present. The second scene (run 8, scene 7) is located in southeastern Florida Bay, an area dominated by open water (relatively large sub-basins) with some very shallow, exposed sediment areas (that effectively separate the sub-basins) and keys (small mangrove islands). No groundtruth data were acquired in this area during the AVIRIS flight.

2.3 Image Processing.

AVIRIS scenes were atmospherically corrected using ATREM (Atmospheric Removal Program) prior to analysis. Image analysis was carried out using ENVI (the Environment for Visualizing Imagery) software. As a preliminary step, each scene was first spectrally sub-sampled to generate a subscene consisting of visible/near IR data (365 to 930 nm). This was accomplished by selecting the first 60 bands (bands 1 through 60) of each individual scene, and removing bands 32 and 33 (at which there is an overlap between two spectrometers). It is this wavelength region in which pigment and sediment data are present.

A spectral library was constructed that included image-derived spectra from pixels associated with each of the seven groundtruth sample stations. The seven stations were imaged on four of the 11 scenes, with single ground-truth stations on three scenes, and four stations in four separate basins on one scene. The latter scene (run 8, scene 10) was the focus of our recent work showing that the discrimination of different phytoplankton assemblages is possible using AVIRIS data (Richardson and Kruse, 1999). The seven image-derived, phytoplankton endmember spectra were supported by groundtruth algal accessory pigment data. Two additional endmember spectra were extracted from the Rankin basin scene (run 5, scene 2) in areas that contained seagrass beds (optically clear water column) and algal mats on the surface of sediment. No groundtruth data were collected at the seagrass and algal mat sites; rather, identification of these pixels as containing endmembers was based on a combination of viewing the imagery and looking for algal mat pigment signatures (see Richardson, 1996). The algal mats also had a sediment signature.

AVIRIS image classifications, using the nine endmember spectra, were conducted using the Spectral Angle Mapper (SAM) algorithm. SAM is an automated method for comparing image spectra to individual spectra (Boardman, unpublished data; Kruse et al., 1993). The algorithm determines the similarity between two spectra by

calculating the "spectral angle" between the two, treating them as vectors in a space with dimensionality equal to the number of bands. The classifications presented in this paper had a maximum SAM angle of 0.20 radians (maximum possible = 2π radians).

3. RESULTS AND DISCUSSION

The image-derived spectra used for AVIRIS image classifications are shown in Figure 1. In this figure the top seven spectra correspond to the seven different phytoplankton assemblages. These spectra were extracted from pixels associated with groundtruth sample sites (seven basins in Florida Bay) at which pigments were sampled during the AVIRIS flight. The bottom two spectra, algal mat/sediment and seagrass, were extracted from an AVIRIS scene (run 5, scene 2, as indicated in Figure 2a) that included these features.

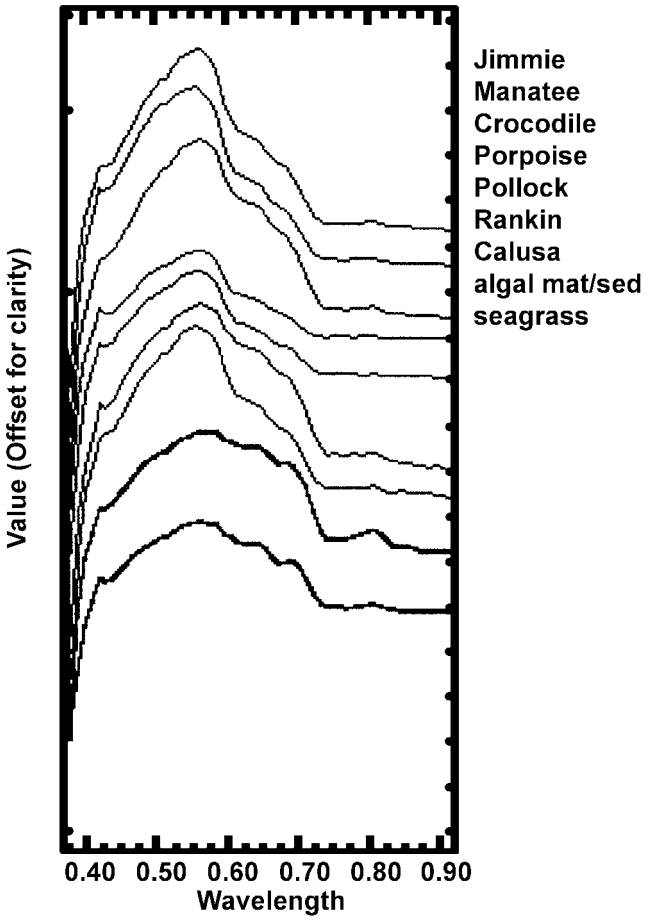

Figure 1. AVIRIS Image-Derived Endmember Spectra.

The seven phytoplankton endmember spectra in Figure 1were supported by the algal accessory pigment data presented in Table 1. These data are part of a much larger (> two year) data set that has been discussed in detail elsewhere (Richardson and Zimba, 2000). The simplified pigment data presented here are limited to chlorophyll *a* and three taxonomically specific accessory pigments: chlorophylls *b* and *c*, and myxoxanthophyll. Chlorophyll *b* is an indicator pigment for green algae. (It is also found in seagrass and all other higher plants.) Myxoxanthophyll is a carotenoid pigment unique to cyanobacteria. Chlorophyll *c* is specific to the Chromophyte algae, which include diatoms and dinoflagellates. In the central/eastern/northern areas of Florida Bay that we are working with, diatoms are the main chl *c* containing phytoplankton group (while dinoflagellates dominate in the west). Thus the data in Table 1 can be interpreted to reveal the type of phytoplankton bloom present in each basin as follows: diatoms only (Calusa); diatoms and cyanobacteria (Pollock, Porpoise, Crocodile, Manatee); diatoms,

Table 1. Algal Pigments Present in Groundtruth Basins in Florida Bay.

Basin	Chlorophyll *a*	Chlorophyll *b*	Chlorophyll *c*	Myxoxanthophyll
Calusa	0.39 µg/l	0	0.14 µg/l	0
Pollock	0.42 µg/l	0	0.14 µg/l	0.06 µg/l
Porpoise	0.36 µg/l	0	0.12 µg/l	0.06 µg/l
Crocodile	0.83 µg/l	0	0.18 µg/l	0.07 µg/l
Manatee	0.53 µg/l	0	0.07 µg/l	0.06 µg/l
Jimmie	0.80 µg/l	0.13 µg/l	0.13 µg/l	0.08 µg/l
Rankin	0.88 µg/l	0.30 µg/l	0.25 µg/l	0.10 µg/l

cyanobacteria and green microalgae (Jimmie and Rankin).

In addition to the three different types of phytoplankton assemblages, there were some differences in the relative proportions of phytoplankton type in the six mixed assemblages. Thus the two basins with three major groups of phytoplankton present (diatoms, cyanobacteria, and green algae) differed in that Rankin had relatively more green algae and diatoms than Jimmie. Rankin also had a high component of suspended sediment (observation). Four of the basins had a mixture of diatoms and cyanobacteria (Pollock, Porpoise, Crocodile, and Manatee). Of these, Crocodile had the highest overall concentration of phytoplankton (as revealed by the relative amount of chl *a*). Pollock and Porpoise had the highest ratios of diatoms to cyanobacteria, as evidenced by the relative amounts of chlorophylls *c* and *a*. Manatee had the lowest proportion of diatoms. For a detailed discussion of the interpretation of pigments in Florida Bay, with additional data including phytoplankton enumeration (microscopic cell identifications and counts) see Richardson and Zimba, 2000.

The two AVIRIS scenes used for SAM classification are shown in Figure 2. Here the scenes are presented as grayscale outputs of three-band composite images (bands 8, 20, and 35, centered at 439, 557 and 685 nm respectively). Figure 1A indicates the location of the Rankin groundtruth sample station (arrow) in Rankin basin as well as the two areas of the image where the seagrass and algal mat endmember spectra were extracted. There were no groundtruth stations sampled in scene 2B.

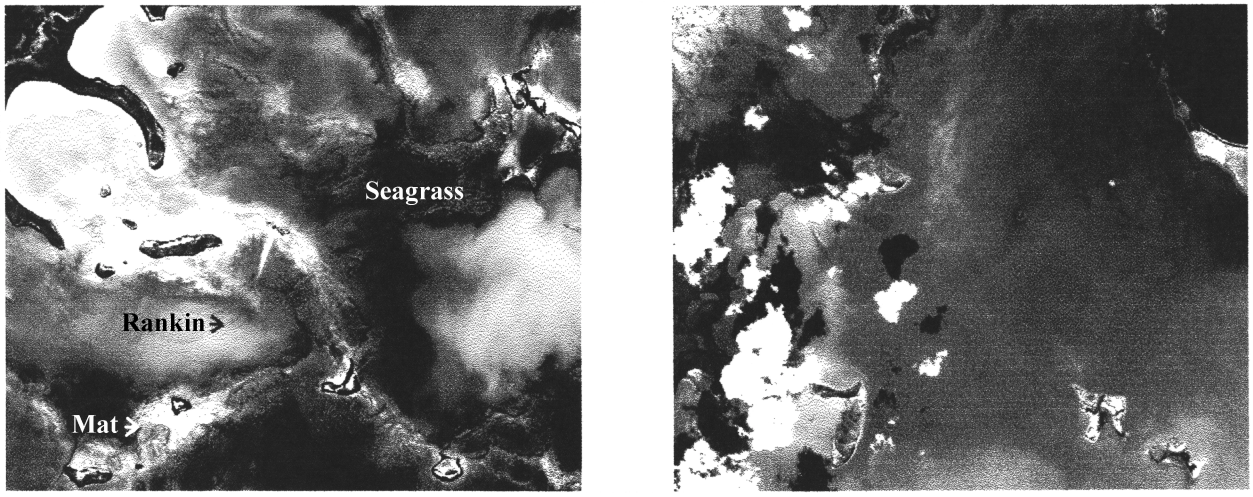

A **B**

Figure 2. Unclassified AVIRIS Scenes. (A = run 5, scene2. B = run 8, scene 7.)

Figures 3 and 4 present classification results of the scenes shown in 2A and 2B respectively. Figures 3A and 4A show SAM classification outputs in which classes were combined to present the distribution of the three major data targets – algal mat/sediment, seagrass beds, and phytoplankton. Both Figures 3 and 4A are classified with the same grayscale class code. Thus in each figure, phytoplankton are classified as black (with the seven

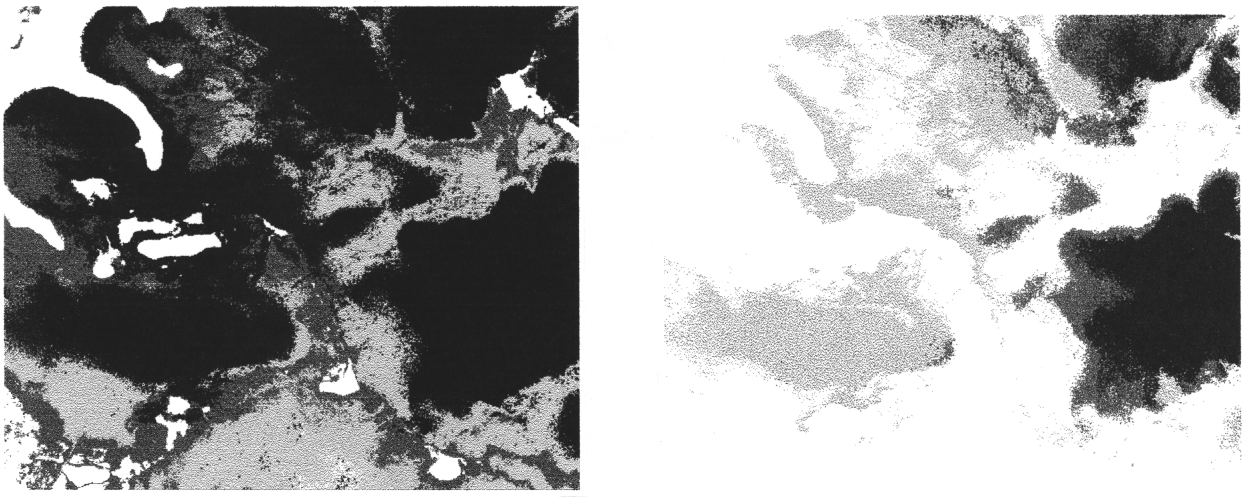

A Seagrass (light gray), mat (gray), phytoplankton (black)

B. Phytoplankton classes (see text)

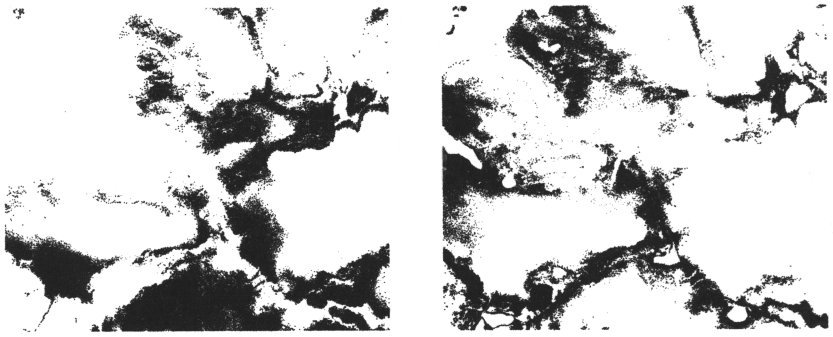

C. Seagrass

D. Algal mat/sediment

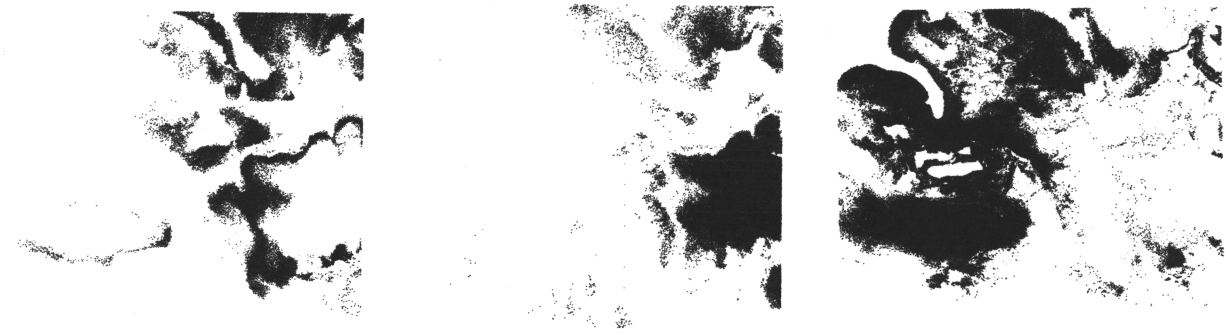

E. Diatoms

F. Diatoms and cyanobacteria

G. Diatoms, cyanobacteria, greens

Figure 3. SAM Classifications (see text). Classified pixels = grayscales and black; unclassified = white.

phytoplankton classes combined); seagrass is light gray; and algal/sediment mat is medium gray. (Unclassified pixels are white.)

Figures 3 and 4 C through G (B is discussed below) show the distributions of the three targets in more detail. The distribution of seagrass is shown (black pixels) in Figures 3 and 4C, while algal mat/sediment (black pixels) are depicted in 3 and 4D. Figures 3 and 4 E, F and G reveal the distributions of the three main phytoplankton taxonomic assemblages (combined in A). Thus in E only diatoms (Calusa class) are depicted. Diatoms and cyanobacteria (four combined classes – Pollock, Porpoise, Manatee and Crocodile) are shown

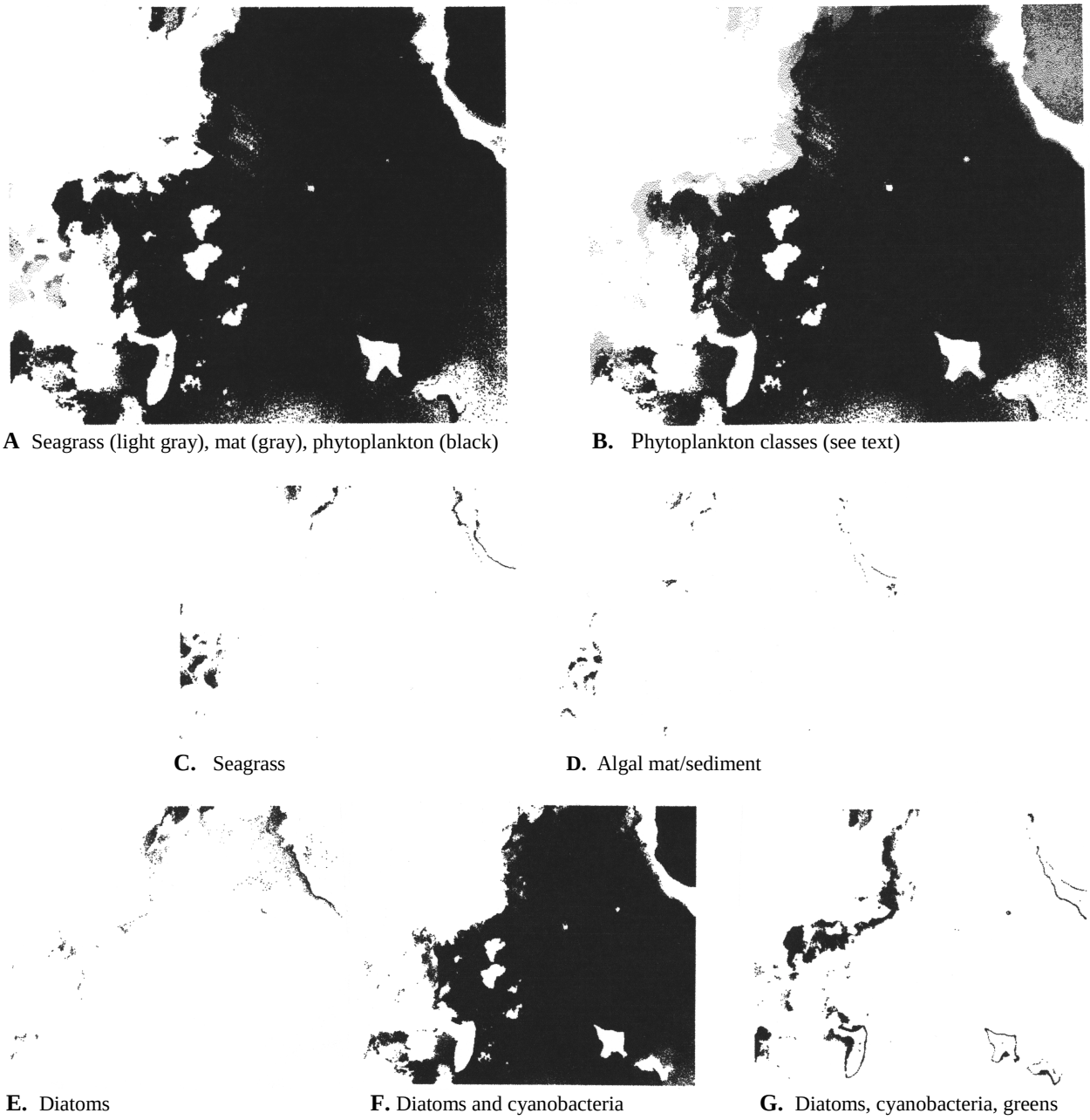

Figure 4. SAM Classifications (see text). Classified pixels = grayscales and black; unclassified = white.

in F; and assemblages with all three phytoplankton (Rankin and Jimmie classes) are shown in G.

Figures 3B and 4B present the classification results of the seven phytoplankton endmembers. In both figures phytoplankton classes are represented as grays and black, and all unclassified, seagrass, and algal mat/sediment pixels are mapped as white. It can be seen that the Rankin scene (3B) had four of the seven different phytoplankton assemblages. The Rankin assemblage itself is mapped as light gray; areas with diatoms only (Calusa endmember) are mapped as medium gray; and two mixtures of diatoms and cyanobacteria (Crocodile and Pollock endmembers) are mapped as black and light/medium gray respectively. Thus it can be seen that the large basin to the right of Rankin basin (compare with Figure 1A) was primarily the Crocodile mixture of diatoms and cyanobacteria (black) with a unialgal diatom bloom around the edges (Calusa class – medium gray).

Figure 4b shows the result of the SAM classification of run 8, scene 7 using the seven phytoplankton endmember spectra. Most of this AVIRIS scene was dominated by a large basin that contained predominately one of the endmember phytoplankton assemblages. This assemblage, classified as black in Figure 4B, corresponds to the Manatee endmember. This assemblage is the mixture of diatoms and cyanobacteria that contained the lowest relative amount of diatoms. The upper right corner of Figure 4B reveals part of another basin that also mapped as a mixture of diatoms and cyanobacteria, but in this case the assemblages matched those of Pollock (medium gray) and Porpoise (dark gray) both of which had the relatively highest ratios of diatoms to cyanobacteria. Along the left edge of the large basin (Manatee class, black pixels) it can be seen that some areas mapped as Rankin (classified as light gray), thus exhibited a mixture of diatoms, cyanobacteria, green algae and suspended sediment.

4. CONCLUSIONS

The results presented here demonstrate that hyperspectral (AVIRIS) data can discriminate between different phytoplankton assemblages and other in-water aquatic organisms (seagrass) dominated by chlorophyll *a*. This was achieved using a spectral based data analysis approach that takes advantage of the spectra present in AVIRIS imagery.

We are just beginning to assess the utility of hyperspectral imaging sensor data for the study of aquatic coastal zones. As more such data become available a next necessary step will be to validate the output of image classifications, especially those identifying phytoplankton classes. Phytoplankton exhibit relatively unstable populations, and it is not valid to assume that any given aquatic body will contain the same population composition over time spans on the order of days. Thus there is a need for groundtruth data acquisition concurrent with hyperspectral image data acquisition to confirm that spectral matches (algorithm outputs) are correct. This is probably not a problem in the work presented here, because the phytoplankton endmember spectra were extracted from the image data and were therefore known spectral constituents of Florida Bay when the AVIRIS imagery was acquired. Although limited to seven stations, the endmember spectra were supported by groundtruth data. Future endeavours, however, will most certainly include classifications of hyperspectral imagery using spectral libraries that contain spectra generated, for example, from laboratory cultures, experimental mesocosms, and spectroradiometer data from other field sites. Positive classification results using such endmembers will have to be confirmed.

Acknowledgments. This research is supported by NASA grant NAG5-8156 to LLR.

5. REFERENCES

Dekker, A. G. and H. J. Hoogenboom, 1996, “Predictive modelling of AVIRIS performance over inland waters,” Sum. 6th JPL Airborne Earth Science Workshop, vol. 1, pp. 83–92.

Dekker, A. G., T. J. Malthus, M. M. Wijnen and E. Sayhan, 1992a, “Remote sensing as a tool for assessing water quality in Loosdrecht lakes,” Hydrobiologia, vol. 233, pp. 137–159.

Dekker, A. G., T. J. Malthus, M. M. Wijnen and E. Seyhan, 1992b, “The effect of spectral bandwidth and positioning on the spectral signature analysis of inland waters,” Rem. Sens. Env., vol. 41, pp. 211–225.

Gitelson, A., 1992, “The peak near 700 nm on reflectance spectra of algae and water: relationships of it’s magnitude and position with chlorophyll concentration,” Intl. J. Rem. Sens. vol. 13, pp. 3367–3373.

Goodin, D. G., L. Han, R. N. Fraser, D. C. Rundquist, W. A. Stebbins and J. F. Schalles, 1993, “Analysis of suspended solids in water using remotely sensed high resolution derivative spectra,” Photogramm. Eng. and Rem. Sens., vol. 59, pp. 505–510.

Han, L., D. C. Rundquist, L. L. Liu, R. N. Fraser and J. F. Schalles, 1994, “The spectral responses of algal chlorophyll in water with varying levels of suspended sediment,” Intl. J. Rem. Sens., vol. 15, pp. 3707–3718.
Kruse, F. A., A. B. Lefkoff, J. B. Boardman, K. B. Heidebrecht, A. T. Shapiro, P. J. Barloon and A. F. H. Goetz, 1993, “The Spectral Image Processing System (SIPS) - Interactive visualization and analysis of imaging spectrometer data,” Rem. Sens. Env., vol. 44, pp. 145–163.

Kruse, F. A., L. L. Richardson and V. G. Ambrosia, 1997, "Techniques developed for geologic analysis of hyperspectral data applied to near-shore hyperspectral ocean data," Proc. Fourth Intl. Conf. Rem. Sens. Marine and Coastal Env., ERIM, vol. 1, pp. 233–246.

Prieur, L. and S. Sathyendranath, 1981, "An optical classification of coastal and oceanic waters based on the specific spectral absorption curves of phytoplankton pigments, dissolved organic matter, and other particulate materials," Limnol. Oceanogr. vol. 41, pp. 671–689.

Richardson, L. L., D. Buisson, C. J. Liu and V. Ambrosia, 1994, "The detection of algal photosynthetic accessory pigments using Airborne Visible-Infrared Imaging Spectrometer (AVIRIS) spectral data," Mar. Technol. Soc. J., vol. 28, pp. 10–21.

Richardson, L. L., 1996, "Remote sensing of algal bloom dynamics," BioScience, vol. 46, pp. 492–501.

Richardson, L. L. and F. A. Kruse, 1999, "Identification and classification of mixed phytoplankton assemblages using AVIRIS image-derived spectra," Proc. 8th JPL Airborne Earth Sciences Workshop, vol. 1, (in press)

Richardson, L. L. and P. V. Zimba, 2000, "Spatial and temporal patterns of phytoplankton in Florida Bay: Utility of algal accessory pigments and remote sensing to assess bloom dynamics," Linkages between Ecosystems in the South Florida Hydroscape: The River of Grass Continues, J. W. Porter and K.G. Porter, (eds.), CRC Press. (in press)

Rowan, K. S., 1989, Photosynthetic Pigments of Algae, Cambridge University Press, Cambridge.

Rundquist, D. C., L. Han, J. F. Schalles and J. S. Peake, 1996, "Remote measurement of algal chlorophyll in surface waters: the case for the first derivative of reflectance near 690 nm." Photogramm. Eng. and Rem. Sens., vol. 62, pp. 195–200.

Schalles, J. F., A. A. Gitelson, Y. Z. Yacobi and A. E. Kroenke, 1998, "Estimation of chlorophyll a from time series measurements of high spectral resolution reflectance in an eutrophic lake." J. Phycol., vol. 34, pp. 383–390.

Schalles, J. F., F. R. Schiebe, P. J. Starks, and W. W. Troeger, 1997, "Estimation of algal and suspended sediment loads (singly and combined) using hyperspectral sensors and integrated mesocosm experiments," Proc. 4th Intl. Conf. Rem. Sens. Marine and Coastal Env. vol, 1, pp. 247–258.

Stumpf, R. P., M. J. Durako, J. W. Fourqurean, V. Ransibrahmanakul and M. L. Frayer, 1999, "Detection of seagrass cover and water clarity in Florida Bay and the Keys," 1999 Florida Bay and Adjacent Marine Systems Science Conference, 211 (abstract).